Applied Surface Science 258 (2012) 6373–6378

Contents lists available at SciVerse ScienceDirect

Applied Surface Science

journal homepage: www.elsevier.com/locate/apsusc

Alteration of Mn exchange coupling by oxygen interstitials in ZnO:Mn thin films

Usman Ilyas[a,b], R.S. Rawat[a,*], Y. Wang[a], T.L. Tan[a], P. Lee[a], R. Chen[c], H.D. Sun[c], Fengji Li[d], Sam Zhang[d]

[a] NSSE, NIE, Nanyang Technological University, 1 Nanyang Walk, 637616 Singapore
[b] Department of Physics, University of Engineering & Technology Lahore, 54890 Pakistan
[c] Division of Physics and Applied Physics, School of Physical and Mathematical Sciences, Nanyang Technological University, 637371 Singapore
[d] School of Mechanical and Aerospace Engineering, Nanyang Technological University, 50 Nanyang Avenue, 639798 Singapore

ARTICLE INFO

Article history:
Received 8 November 2011
Received in revised form 24 January 2012
Accepted 10 March 2012
Available online 17 March 2012

Keywords:
ZnO:Mn thin films
Spin coating technique
Oxygen interstitials
Dilute magnetic semiconductors (DMS)
Room temperature ferromagnetism (RTFM)

ABSTRACT

The un-doped and Mn doped ZnO thin films, with oxygen rich stoichiometry, were deposited onto Si (1 0 0) substrate using spin coating technique. The structural analysis revealed the hexagonal wurtzite structure without any impurity phase formation. A consistent increase in cell volume with the increase in Mn doping concentration confirmed the successful incorporation of bigger sized tetrahedral Mn^{2+} ions (0.83 Å) in ZnO host matrix that was also endorsed by the presence of Mn $2p_{3/2}$ core level XPS spectroscopic peak. Extended deep level emission (DLE) spectra centered at ~627 nm confirmed the presence of oxygen interstitials. Moreover, the magnetic measurements of field dependent *M–H* curves revealed the origin of ferromagnetic ordering from Mn-defect pair exchange coupling with oxygen interstitials in ZnO host matrix.

1. Introduction

Dilute magnetic semiconductors (DMS) have recently attracted tremendous attention due to their possible applications in spintronic devices as the charge and spin of electrons are accommodated into single material for interesting magneto-optical and magneto-electric properties [1,2]. Soon after Dietl's prediction about the room temperature ferromagnetism (RTFM) in ZnO:Mn thin films heavily doped with holes[3], a lot of research work was started on ZnO based DMS. Wide band gap wurtzite phase ZnO is a strong piezoelectric and electro-optic material which with transition metal doping can be used as a multifunctional material in optoelectronics and spintronics [4,5]. There has been a considerable interest in the fabrication of transition metal doped ZnO thin films with RTFM for its implementation in spintronic devices [6]. Numerous studies have therefore been carried out to grow ZnO:Mn thin films due to large magnetic moment exhibited by manganese (Mn) [7,8]. However, one of the main obstacles in creating high quality ZnO-based optoelectronic and spintronic devices, is the unavailability of ferromagnetic ZnO:Mn thin films with significant hole carriers concentration. The main reason behind the difficulty in achieving the p-type conductivity is the presence of structural defects like oxygen vacancies and zinc interstitials which are unintentionally introduced during thin film growth, making ZnO inherently an n-type material. The RTFM in n-type ZnO:Mn thin films is reported to be limited at lower temperatures [9]. Some researchers have addressed this issue by reporting defect mediated RTFM due to zinc and oxygen vacancies [10,11]. In spite of RTFM in ZnO:Mn thin films reported by several groups [12–14], a non ferromagnetic behavior has also been reported in polycrystalline ZnO:Mn thin films at room temperature [15,16]. Subsequently, some researchers reported the origin of ferromagnetism due to impurity phases such as oxides of Mn and spinal phases ($ZnMn_2O_4$) [17]. Due to the controversial results indicated in literature, the origin of ferromagnetism is still in debate and is a matter of great concern. In addition, the lack of reproducibility of ferromagnetic signal in ZnO:Mn thin films prepared with the same manganese content and growth conditions put the question mark on the origin of the ferromagnetism.

In view of controversial results about the origin of RTFM in transition metal doped ZnO, the present paper aims to shed some light on the origin of ferromagnetism in Mn doped ZnO thin films grown by spin coating method. In view of Dietl's prediction [3] about the importance of holes in ZnO:Mn thin films, we report the origin of ferromagnetism in oxygen rich ZnO:Mn thin films to be due to Mn-defect pair ferromagnetic exchange coupling with acceptors (oxygen interstitials). The investigation of ZnO:Mn based DMS to optimize the synthesis and growth parameters of Mn doped ZnO nanocrystalline thin films is useful for spintronic applications.

* Corresponding author. Tel.: +65 6790 3930/6790 3908; fax: +65 6896 9414.
E-mail address: rajdeep.rawat@nie.edu.sg (R.S. Rawat).

0169-4332/$ – see front matter © 2012 Elsevier B.V. All rights reserved.
doi:10.1016/j.apsusc.2012.03.043

2. Experimentation

Mn doped ZnO thin films with wurtzite structure were synthesized using spin coating technique. The Mn-doped ZnO thin films were prepared for four different Mn doping concentrations of 0, 2, 5 and 10 at.% hereinafter referred as SG0%, SG2%, SG5% and SG10%, respectively. Zinc acetate dihydrate (90 mMol) and manganese acetate tetrahydrate (2.9 mMol) were mixed along with potassium hydroxide (280 mMol) at room temperature in an environment of methanol (50 ml) for the preparation of SG2% sample. The solution was continuously stirred using a magnetic stirrer for 3 h at 52 °C to get homogeneous mixing in solution. It was then cooled to room temperature and was allowed to age for 24 h. Similar coating solutions for thin films of SG5% and SG10% were prepared by the same procedure using suitable quantities of acetates and solvents. The thin films of these solutions were coated on Si (1 0 0) substrate at 3000 rev/min for 30 s using 6708D Desk-Top Precision Spin Coating System. After deposition with spin coater, the thin films were dried at 100 °C for 5 min. The procedure from coating to drying was repeated 5–8 times to reach the desired thickness of ~150 nm. The thin films were then annealed in air at 550 °C for 2 h to improve their crystalline quality.

The structural properties regarding the crystallinity of the thin films were analyzed using SIEMENS D5005 Cu K_α (1.504 Å) X-ray Diffractometer (XRD). Near band edge (NBE) and deep level emission (DLE) energy transitions in photoluminescence (PL) spectra, obtained using Hd–Cd (325 nm, 10 mW) laser as an excitation source, were used to study the variations in optical band gap and structural defects with varying Mn doping concentration. Kratos Axis-Ultra Spectrometer equipped with a focused monochromatic Al-K_α (1486.6 eV) X-ray beam (15 kV and 10 mA) was employed for X-ray photoelectron spectroscopy (XPS) to identify the surface stoichiometry and elemental oxidation states in Mn doped ZnO thin films. Surface morphology of the thin films along with the quantitative analysis of elements was characterized using a JEOL JSM 6700 field emission scanning electron microscope (FESEM) coupled with Oxford Instrument's energy dispersive X-ray (EDX) System. Furthermore, the field dependent magnetic characterization was performed using Lakeshore 7404 vibrating sample magnetometer (VSM) at room temperature to study the ferromagnetic ordering in ZnO:Mn thin films.

3. Results and discussion

3.1. XRD analysis

The XRD spectra of $Zn_{1-x}Mn_xO$ thin films for different Mn doping concentrations (x = 0.00, 0.02, 0.05 and 0.10) are shown in Fig. 1. The XRD profiles, showing hexagonal wurtzite structure, were matched well with space group $P6_3mc$ (no. 186) (ICSD # 82028) of wurtzite ZnO and no signatures of any impurity or binary zinc-manganese phase (including oxides of Mn and spinal phases) were observed. So the occurrence of impurity phases such as the oxides of Mn and spinal phase is ruled out in any of the doped samples. The texture coefficient of ZnO:Mn thin films was estimated to determine the preferred orientation of polycrystalline thin films using the formula proposed by Barret and Massalski [18]. The (1 0 1) peak was found

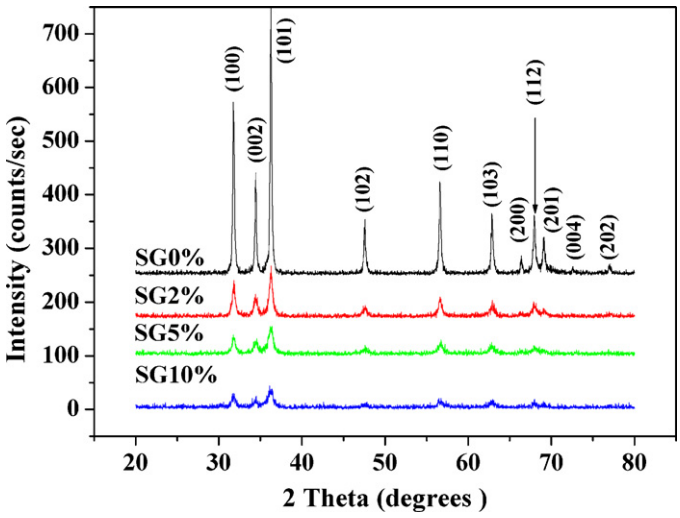

Fig. 1. XRD spectral profiles of un-doped and Mn-doped ZnO thin films.

to have higher texture coefficient indicating the preferred orientation of the thin films along this plane. Hence, the parameters such as diffraction peak shift, lattice parameters and lattice volume of ZnO:Mn thin films have been estimated for this peak. The lattice parameters, listed in Table 1, were estimated using the plane-spacing equation for hexagonal wurtzite structure of ZnO and the Bragg's equation. Highly textured peak centered at ~36.2° (characterizing the hexagonal wurtzite structure) was shifted toward smaller angles (indicating increasing d-spacing) with the increase in Mn doping content (refer Table 1). This peak shift suggests the incorporation of larger sized (0.83 Å) tetrahedral Mn^{2+} ions at the substitutional lattice sites of Zn^{2+} (0.74 Å) ions [19] resulting in increased interlayer spacing (d-spacing). In addition, the diffraction peak broadening (increase in FWHM) with increase in Mn content can be attributed to the decrease in average crystallite size and/or to the strain induced from the incorporation of Mn ions at Zn ion sites (size mismatching). The average crystallite sizes of the samples, determined from the FWHM of the diffraction peak centered at ~36.2° using Scherer formula, were estimated to be 17.01, 8.81, 7.01 and 6.17 nm for SG0%, SG2%, SG5% and SG10%, respectively. The lattice parameter 'a' and cell volume increased consistently with the increase in Mn content, as seen in Table 1, while the trend in variation of lattice parameter 'c' was inconsistent. The cell expansion reflects the incorporation of larger Mn^{2+} cations (0.83 Å) at the substitutional sites of Zn^{2+} (0.74 Å), without any degradation in the wurtzite crystal structure of host ZnO matrix.

3.2. PL analysis

PL spectra of un-doped and Mn doped ZnO thin films exhibit two emission bands in UV and visible (mostly in yellow spectral region) regions, as shown in Fig. 2. The UV emission peak, centered at ~376–384 nm (3.24–3.30 eV) for different Mn doping concentrations, originates from the radiative exciton recombination corresponding to the NBE exciton emission of the wide band gap ZnO. The intensity of the UV emission peak (refer Fig. 2) strongly

Table 1
FWHM and cell volume of ZnO:Mn thin films.

Sample name	Center of peak	FWHM	d-Spacing (Å)	Lattice parameter a (Å)	Lattice parameter c (Å)	Cell volume (Å^3)
SG0%	36.264	0.008554	2.4752	3.2489	5.2049	47.579
SG2%	36.261	0.016541	2.4754	3.2493	5.2047	47.588
SG5%	36.248	0.020784	2.4763	3.2509	5.2018	47.609
SG10%	36.209	0.023618	2.4788	3.2534	5.2062	47.722

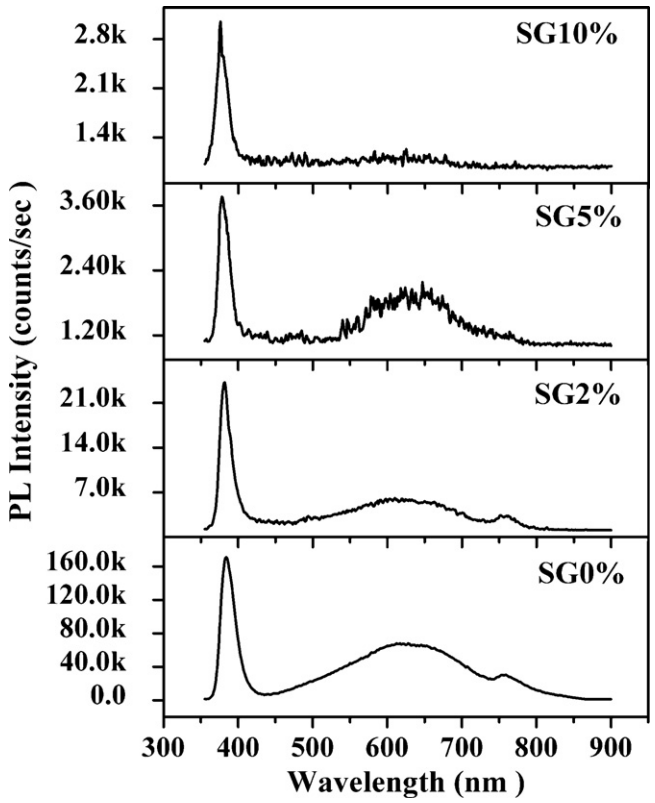

Fig. 2. PL emission spectra of un-doped and Mn doped ZnO thin films.

depends on the Mn content and decreases with the increase in Mn content that might be attributed to some non radiative recombination processes [20].

The UV emission peak shifts toward the shorter wavelength side (blue shift) from 383.6 to 375.9 nm with the increase in Mn content, as is evident from Fig. 2. The observed blue shift in UV emission peak is a result of increased optical band gap of ZnO host matrix. The increased optical band gap (blue shift) is attributed to the reduced average crystallite size [21] of Mn doped ZnO thin films as estimated and discussed in XRD results Section 3.1.

The DLE spectra, which strongly manifest a polycrystalline structure of ZnO, is due to structural defects such as Zn vacancy (V_{Zn}), oxygen vacancy (V_o), interstitial zinc (Zn_i) and interstitial oxygen (O_i) [22]. From Fig. 2, it is evident that the structural defects are significantly reduced with the increase in Mn content as indicated by the marked decrease in the DLE peak intensity centered at about 624–633 nm. The relative contributions of different native defects in DLE spectra can be evaluated by the estimation of relative intensities of the deconvoluted peaks. The deconvoluted DLE peak was found to be fitted, mainly, by two peaks centered at about ~627 and 736 nm. The peak at ~736 nm is the second order reflection of the UV peak. The deconvoluted DLE spectral peak centered at ~627 nm is attributed to the presence of O_i. The presence of O_i (acceptor defects) and the absence of DLE emission peak corresponding to oxygen vacancy in all the thin films indicate that the oxygen is not self-interstitial rather our samples are oxygen rich. The oxygen rich stoichiometry of the samples is also verified by EDX results, discussed later in Section 3.4. Among all the doped thin films under investigation, SG5% was found to have maximum concentration of O_i (66.5%). The presence of O_i, due to oxygen rich stoichiometry in all thin film samples, in turn is favorable to exhibit p-type conductivity due to the activation of acceptor states, as is reported in our previous study [23]. The activation of acceptor states for hole formation is responsible for an enhancement in RTFM in this sample, as discussed later in Section 3.5, that is consistent with the Dietl's prediction [3] of holes mediated ferromagnetism in Mn doped ZnO thin films. The reduced value of acceptors (O_i) in SG10% (34%) indicates the increased carrier concentration of donors (electrons) which in turn suppressed the ferromagnetic ordering for this sample, as discussed later in Section 3.5.

3.3. XPS analysis

The compositional analysis of ZnO:Mn thin films was performed by investigating the Zn 2p, Mn 2p and O 1s core level XPS spectra after calibrating their binding energies by adventitious C 1s peak (284.6 eV) as a reference. The stoichiometery of ZnO:Mn thin films calculated from the relative area under curve of the zinc and oxygen peaks, after a Shirley background subtraction by non linear least square fitting using mixed Gauss–Lorentz function, is found to be oxygen rich with Zn/O < 1 for all the thin films.

The typical Zn $2p_{3/2}$ core level XPS spectrum of SG10% is shown in Fig. 3. The asymmetric Zn $2p_{3/2}$ peak of zinc in the elemental as well as oxide forms usually consists of two peaks centered at ~1021.5 and ~1022.4 eV respectively [24]. In our case, the main XPS spectrum of SG10% exhibits, upon deconvolution using Gaussian function, core level binding energy peaks of Zn $2p_{3/2}$ at ~1020.4 eV and ~1021.8 eV (refer Fig. 3(a)). The lower energy peak centered at ~1020.4 eV is attributed to the O^{2-} ions in the wurtzite structure of the hexagonal Zn^{2+} ion array i.e. the oxide form of Zn in ZnO [25], while the peak centered at ~1021.8 eV is attributed to the metallic zinc. Higher intensity of lower energy peak suggests that the majority of Zn atoms in ZnO host matrix are in Zn^{2+} state. The deconvoluted peaks are found to shift toward the lower binding energy values as compared to the values reported in literature [26] which can be attributed to the partial substitution of lattice by Mn^{2+} ions in ZnO and Zn—Mn bonding structure [27]. Since the electro negativity of Mn ($\chi = 1.55$) is smaller than that of O ($\chi_o = 3.44$) [28], Zn atoms bonded to the Mn atoms will contribute to the shift in the binding energy of Zn $2p_{3/2}$. Furthermore, the reduced crystallite size which broadens the peak also contributes to the shift in binding energy toward lower energy side [25]. Similar trends were observed for other thin film samples.

Fig. 3(b) shows Mn 2p core level XPS spectrum of SG10% sample fitted with deconvoluted peaks centered at ~640.3 and ~654.0 eV estimated using Gaussian peak fitting. It can be seen from Fig. 3(b) that each main peak has satellite peak on the higher binding energy side. Similar spectra were obtained for all other samples. The first peak centered at ~640.3 eV confirms the presence of Mn^{2+} in the host ZnO lattice [29]. The contribution of this peak, estimated from the relative area under curve, increases with the increase in Mn content which in turn validates the enhanced concentration of Mn^{2+} in higher doped samples.

Fig. 3(c) shows the asymmetric O 1s peak of SG10%, deconvoluted with peaks centered at ~529.8, 531.3 and 531.9 eV respectively. Similar spectral features were observed for all other thin film samples. The lower energy peak is attributed to the O^{2-} ions in the wurtzite structure of the hexagonal Zn^{2+} ion array which can be attributed to Zn—O bonds [30]. The contribution of oxygen in Zn—O bonds estimated from the relative area under curve of peak at ~529.8 eV was observed to be 47, 55, 80 and 49% for SG0%, SG2%, SG5% and SG10% thin film samples, respectively. Maximum value (80%) in SG5% reveals an enhanced concentration of oxygen in Zn—O bonding that in turn indicates minimum concentration of V_o in SG5%. This was further validated by estimating the relative contribution of V_o (donor defects) from the relative area under curve of the peak centered at ~531.3 eV; and was found to be 33, 23, 7 and 45% for SG0%, SG2%, SG5% and SG10% samples, respectively. Moreover, the component of binding energy centered at ~531.9 eV is associated with the presence of chemisorbed

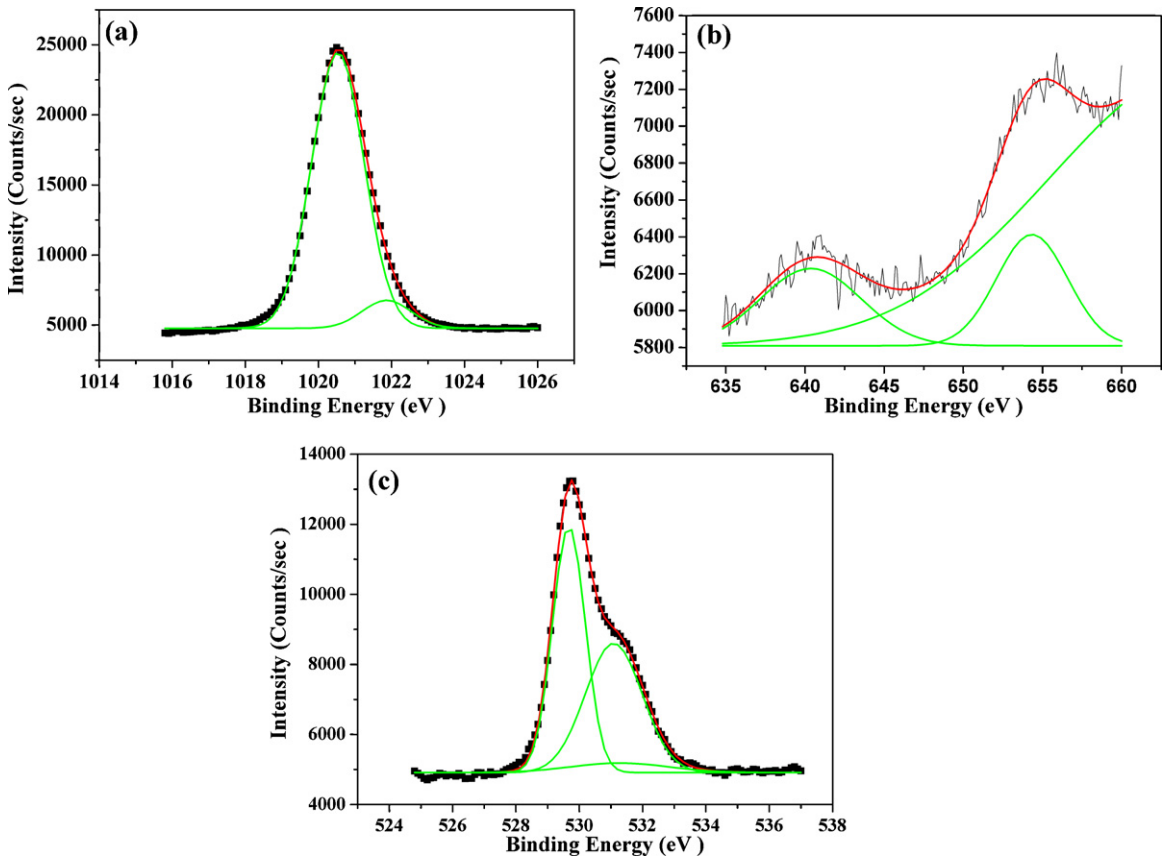

Fig. 3. Deconvoluted core level XPS spectra of (a) Zn $2p_{3/2}$ (b) Mn 2p, and (c) O 1s of SG10% sample.

oxygen within the ZnO host matrix. The presence as well as variations in the area under curve for this component may be, in part, related to the variation in oxygen interstitials [31] which is consistent with our PL results.

3.4. Morphological studies

Fig. 4a shows the FESEM micrograph exhibiting the cracks in the thin films after annealing. The cracks in the thin films are possibly due to different expansion coefficients of Si and ZnO, which increases the surface roughness of the thin films. The typical EDX spectrum of SG5% with elemental compositional analysis, shown in Fig. 4b, exhibits the presence of Mn, though at lower atomic percentage as compared to the doping concentration. The EDX quantitative measurement shows 2.01 at.% Mn in SG5% sample while the actual doping concentration was 5 at.%. The EDX analysis showed that the amount of Mn incorporation increased with the increase in Mn concentration and also revealed the dominance of oxygen in all the samples exhibiting oxygen rich stoichiometry of thin films as observed in XPS results as well.

3.5. VSM analysis

Fig. 5 reveals the dependence of magnetization (M) with applied magnetic field (H) for ZnO:Mn thin films. The field dependence of magnetization at room temperature for un-doped and Mn-doped ZnO thin films is studied in the magnetic field range of 0–3000 G. The actual magnetic signal of all the doped thin films was determined by subtracting the contribution of Si substrate and diamagnetic signal of un-doped ZnO from the raw data. The typical magnetization of all the doped thin films is strongly dependent on Mn doping concentration, as shown in Fig. 5. The M–H curve

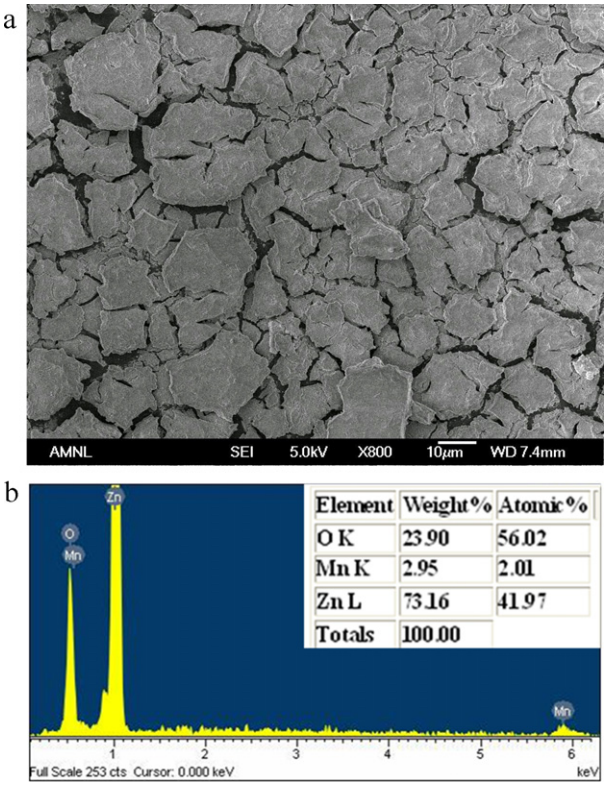

Fig. 4. FESEM micrograph, along with EDX spectra showing elemental concentration, of SG5% sample.

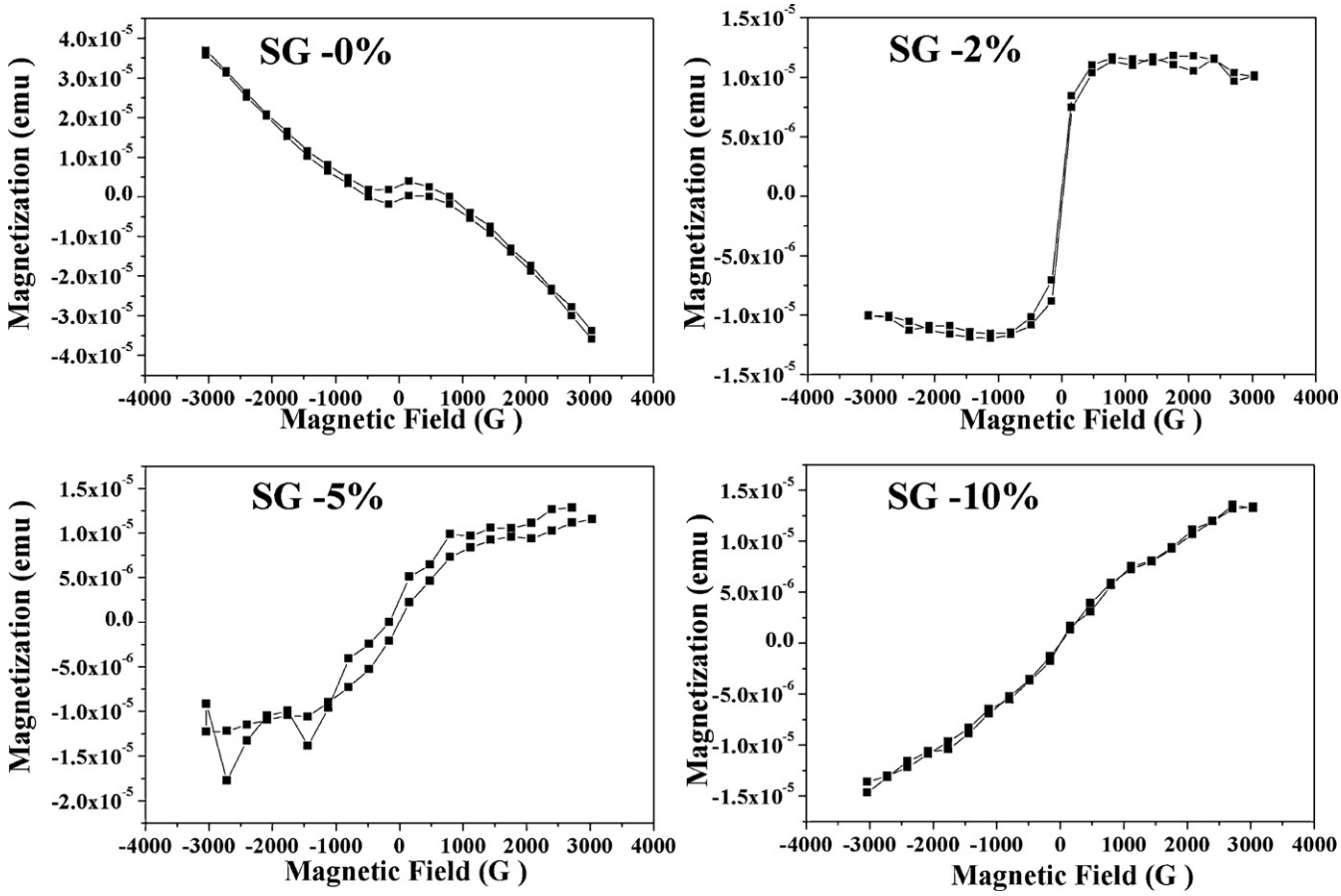

Fig. 5. Field dependent *M–H* curves of un-doped and Mn-doped ZnO thin films.

of SG0% shows the diamagnetic behavior while the *M–H* curves of SG2% and SG5% exhibit RTFM with the exception of SG10% in which the paramagnetic phase is dominant (refer Fig. 5). The diamagnetic behavior of SG0% samples also suggests that the ferromagnetic signal in SG2% and SG5% is solely due to the presence of Mn ions in ZnO host matrix. The values of saturation magnetization and coercive field corresponding to SG2% and SG5% are 11.97 μemu and 13.70 G, and 15.15 μemu and 82.22 G, respectively. These values along with the shape of *M–H* curve suggest the presence of weak ferromagnetism, soft magnetic phase, in SG2% and SG5% samples. The maximum value of saturation magnetization was achieved for SG5% sample but it is much smaller than the reported value of Mn^{2+} state [10]. The reduced value of saturation magnetization might be attributed to the direct Mn–Mn anti-ferromagnetic exchange coupling between the neighboring Mn atoms that reduce the ferromagnetic signal.

According to the bound magnetic polaron (BMP) model, bound electrons in the defect states can couple with Mn ions and cause the ferromagnetic regions to overlap, giving rise to long range ferromagnetic ordering in the thin films [11]. In accordance with the BMP model, the magnetization of the system originates from the regions of correlated and isolated spins. The magnetization that arises from correlated spins is ferromagnetic (M_{FM}), whereas the magnetization that is due to the uncorrelated spins is paramagnetic (M_P) [11]. If specific intrinsic point defect of ZnO has the main contribution toward the ferromagnetism in ZnO:Mn thin films, it should have the same trend as that of *M–H* curves shown in Fig. 5. The trend of variation in O_i concentration is consistent with the trend of *M–H* curves in doped thin films. The concentration of oxygen interstitials was estimated to be maximum for SG5% and minimum for SG10% (refer to PL analysis in Section 3.2) that is consistent with the ferromagnetic trend shown in Fig. 5 in which the saturation magnetization for SG5% was observed to be maximum. The O_i (acceptors) might have strong correlated spins and can form extended molecular orbits around the defect site, which couple ferromagnetically. Moreover, the probable indirect Mn–O–Mn exchange coupling led by the O_i might also be the possible reason for stabilizing long range RTFM in ZnO:Mn thin films. So based on the above discussion, it can be concluded that maximum concentration of O_i in SG5% is responsible for correlated spins leading to enhanced RTFM in this sample, while the minimum concentration of O_i in SG10% sample might not be sufficient to overcome the uncorrelated spins of isolated Mn atoms and therefore retains the paramagnetic phase. The increased value of saturation magnetization and maximum concentration of O_i (acceptor defects) in SG5% (refer to PL analysis in Section 3.2) validates the acceptors (holes) induced RTFM that is in accordance with Dietl's prediction.

Furthermore, in SG10%, the decreasing average distance between the adjacent Mn atoms due to increased concentration of Mn (10 at.%) will favor super exchange Mn–Mn interaction, which is believed to be anti-ferromagnetic [32] due to overlapping of Mn d-states with the valence band. As the anti-ferromagnetic energy is lower than the ferromagnetic one due to the reduced distance between the adjacent Mn ions, most of Mn atoms should be anti ferromagnetically coupled at the relatively higher Mn concentrations (10 at.% Mn). Due to the direct anti-ferromagnetic exchange coupling and competitions between d-shells of adjacent Mn ions, the ferromagnetic signals exhibited due to indirect exchange coupling are suppressed in SG10%.

4. Conclusions

Oxygen rich nanocrystalline ZnO:Mn thin films were prepared through a relative simple spin coating technique. The solutions for spin coating of thin films were prepared through wet chemical route by mixing suitable quantities of zinc acetate dihydrate, manganese acetate tetrahydrate, potassium hydroxide in an environment of methanol. The XRD measurements revealed the nanocrystalline nature of ZnO:Mn thin films with a consistent increase in lattice parameter '*a*' and cell volume with the increase in Mn doping concentration. The cell expansion in Mn doped nanocrystalline thin films confirmed the successful incorporation of larger sized (0.83 Å) tetrahedral Mn^{2+} ions at the lattice sites of Zn^{2+} ions (0.74 Å) in ZnO host matrix. The detailed XPS analysis of Zn 2p, Mn 2p and O 1s core level spectra revealed the incorporation of Mn^{2+} at the lattice sites of Zn with marked decrease in oxygen vacancies in higher doped samples. NBE emission spectra in PL revealed the UV peak shift toward the shorter wavelength side with increasing Mn concentration resulting in enhanced optical band gap. Extended DLE spectra showing the signatures of oxygen interstitials (acceptors) in yellow emission band endorsed the hole induced RTFM in ZnO:Mn thin films. The maximum contribution of O_i in SG5% favored Mn-defect pair indirect exchange coupling resulting in RTFM. Their increased concentration conferred the random distribution of Mn ions with uncorrelated spins leading to dominant paramagnetic phase in SG10%. The controlled Mn doping in ZnO thin films therefore led to RTFM and enhanced optical transmission properties in ZnO thin films.

Acknowledgments

This project was supported by the AcRF grant (RI 7/08 RSR) provided by NIE, Nanyang Technological University Singapore. One of the authors, Usman Ilyas, is grateful to the University of Engineering & Technology Lahore for providing fully funded research scholarship under faculty development program (FDP) of Higher Education Commission (HEC) of Pakistan.

References

[1] S.A. Wolf, D.D. Awschalom, R.A. Buhrman, J.M. Daughton, S.V. Molnar, M.L. Roukes, A.Y. Ctchelkanova, D.M. Treger, A spin-based electronics vision for the future, Science 294 (2001) 1488–1495.
[2] H. Ohno, Making nonmagnetic semiconductors ferromagnetic, Science 281 (1998) 951–956.
[3] T. Dietl, H. Ohno, F. Matsukura, J. Cibert, D. Ferrand, Zener model description of ferromagnetism in zinc-blend magnetic semiconductors, Science 287 (2000) 1019–1022.
[4] Y. Caglar, S. Ilican, M. Caglar, Influence of Mn incorporation on the structural and optical properties of sol gel derived ZnO film, J. Sol–Gel Sci. Technol. 53 (2010) 372–377.
[5] Y. Liu, S. Yang, Y. Zhang, D. Bao, Influence of Mn-doped ZnO thin films prepared by sol–gel method, J. Magn. Magn. Mater. 321 (2009) 3406–3410.
[6] L. Ren, Y.J. Won, Effect of temperature and nickel content on magnetic properties of Ni-doped ZnO, Rare Metals 25 (2006) 24–29.
[7] D.S. Reddy, S.K. Sharma, Y.D. Reedy, B.S. Reddy, K.R. Gunasekhar, P. Sreedhara Reddy, Structural and photoluminescence properties of $Zn_{1-x}Mn_xO$ nanoparticles for optoelectronic device applications, J. Optoelectron. Adv. Mater. 10 (2008) 2607–2610.
[8] A.M. Abdel Hakeem, Room-temperature ferromagnetism in $Zn_{1-x}Mn_xO$, J. Magn. Magn. Mater. 322 (2010) 709–714.
[9] R.P. Davies, C.R. Abernathy, S.J. Pearton, D.P. Norton, M.P. Ivill, F. Ren, Chem. Eng. Commun. 196 (2009) 1030–1053.
[10] S. Chattopadhyay, S.K. Neogi, A. Sarkar, M.D. Mukadam, S.M. Yusuf, Defects induced ferromgnetism in Mn doped ZnO, J. Magn. Magn. Mater. 323 (2011) 363–368.
[11] M. El-Hilo, A.A. Dakhel, Structural and magnetic properties of Mn-doped ZnO powders, J. Magn. Magn. Mater. 323 (2011) 2202–2205.
[12] Y.Q. Chang, D.B. Wang, X.H. Luo, et al., Synthesis, optical and magnetic properties of diluted magntic semiconductor $Zn_{1-x}Mn_xO$ nanowires via vapor phase growth, Appl. Phys. Lett. 83 (2002) 4020–4022.
[13] D.B. Norton, S.J. Pwarton, A.F. Hebard, et al., Ferromagntism in Mn-implanted ZnO:Sn single crystals, Appl. Phys. Lett. 82 (2003) 239–241.
[14] A.K. Pradha, K. Zhang, S. Mohantry, et al., High-temperature ferromagnetism in pulsed laser deposited expitaxial (Zn, Mn)O thin films: effects of substrate temperature, Appl. Phys. Lett 86 (2005) 152511.
[15] S.S. Kim, J.H. Moon, B.T. Lee, O.S. Song, J.H. Je, Hetreptaxial growth behavior of Mn-doped ZnO thin films on Al_2O_3 (0 0 0 1) by pulsed laser deposition, J. Appl. Phys. 95 (2004) 454–459.
[16] T. Fukumura, Z. Jin, M. Kawasaki, T. Shono, T. Hasegawa, S. Koshihara, H. Koinuma, Magnetic properties on Mn-doped ZnO, Appl. Phys. Lett. 78 (2001) 958–960.
[17] J.H. Li, D.Z. Shen, J.Y. Zhang, D.X. Zhao, B.S. Li, Y.M. Lu, Y.C. Liu, X.W. Fan, Magnetism origin of Mn-doped nanoclusters, J. Magn. Magn. Mater. 302 (2006) 118–121.
[18] C. Barret, T.B. Massalski, Structure of Metals, Pergamon, Oxford, 1980.
[19] J. Anghel, A. Thurber, D.A. Tenne, C.B. Hanna, A. Punnoose, Correlation between saturation magnetization, bandgap, and lattice volume of transition metal, M = Cr, Mn, Fe, Co, or Ni doped $Zn_{1-x}M_xO$ nanoparticles, J. Appl. Phys. 107 (2010) 09E314.
[20] X.T. Zhang, Y.C. Liu, J.Y. Zhang, Y.M. Lu, D.Z. Shen, X.W. Fan, X.G. Kong, Structure and photoluminescence of Mn-passivated nanocrystalline ZnO thin films, J. Cryst. Growth 254 (2003) 80–85.
[21] C.R. Marotti, P. Giorgi, G. Machado, E.A. Dalchiele, Crystallite size dependence of band gap energy for electrodeposited ZnO grown at different temperatures, Solar Energy Mater. Solar Cells 90 (2006) 2356–2361.
[22] Usman Ilyas, R.S. Rawat, G. Roshan, T.L. Tan, P. Lee, S.V. Springham, Sam Zhang, Li Fengji, R. Chen, H.D. Sun, Quenching of surface traps in Mn doped ZnO thin films for enhanced optical transparency, Appl. Surf. Sci. 258 (2011) 890–897.
[23] Usman Ilyas, R.S. Rawat, T.L. Tan, P. Lee, R. Chen, H.D. Sun, Li Fengji, Sam Zhang, Oxygen rich p-type ZnO thin films using wet chemical route with enhanced carrier concentration by temperature-dependent tuning of acceptor defects, J. Appl. Phys. 110 (2011) 093522.
[24] K.G. Saw, K. Ibrahim, Y.T. Lim, M.K. Chai, Self-compensation in ZnO thin films: an insight from Z-ray photoelectron spectroscopy, Raman spectroscopy and time-of-flight secondary ion mass spectroscopy analyses, Thin Solid Films 515 (2007) 2879–2884.
[25] Y.Y. Taya, S. Lib, C.Q. Sun, P. Chen, Size dependence of Zn 2p3/2 binding energy in nanocrystalline ZnO, Appl. Phys. Lett. 88 (2006) 173118.
[26] S. Karamat, S. Mahmood, J.J. Lin, Z.Y. Pan, P. Lee, T.L. Tan, S.V. Springham, R.V. Ramanujan, R.S. Rawat, Structural, optical and magnetic properties of $(ZnO)_{1-x}(MnO_2)_x$ thin films deposited at room temperature, Appl. Surf. Sci. 254 (2008) 7285–7289.
[27] C.J. Cong, L. Liao, J.C. Li, L.X. Fan, K.L. Zhang, Nanotechnology 16 (2005) 981–984.
[28] W. Xiao, Q. Chen, Y. Wu, T. Wu, L. Dai, Ferromagnetism of $Zn_{0.95}Mn_{0.05}O$ controlled by concentration of zinc acetate in ionic liquid precursor, Mater. Chem. Phys. 123 (2010) 1–4.
[29] S.R. Sarath Kumar, M. Nejib Hedhili, H.N. Alshareef, S.K. Asiviswanathan, Correlation of Mn charge state with the electrical resistivity of Mn doped indium tin oxide thin films, Appl. Phys. Lett. 97 (2010) 111909.
[30] P.T. Hsieh, Y.C. Chen, K.S. Kao, C.M. Wang, Luminescence mechanism of ZnO thin film investigated by XPS measurement, Appl. Phys. A: Mater. Sci. Process. 90 (2008) 317–321.
[31] Usman Ilyas, R.S. Rawat, T.L. Tan, P., Lee, R., Chen, H.D. Sun, Li Fengji, Sam Zhang, Enhanced indirect ferromagnetic p–d exchange coupling of Mn in oxygen rich ZnO:Mn nanoparticles synthesized by wet chemical method, J. Appl. Phys. 111 (2012) 033503.
[32] D. Iusan, B. Sanyal, O. Eriksson, Theoretical study of the magnetism of Mn-doped ZnO with and without defects, Phys. Rev. B 74 (2006) 235208.